*35th EPS Conference on Plasma Phys. Hersonissos, 9 - 13 June 2008 ECA Vol.**32D**, P-1.102 (2008)*

ELECTRON CYCLOTRON HEATING SECOND HARMONIC MODELLING WITH FULL WAVE CODE IN MIDDLE TOKAMAKS AND ITER

V.Vdovin
RRC Kurchatov Institute, Nuclear Fusion Institute

We present modelling results of basic Electron Cyclotron Heating scenarios in tokamaks performed with newly developed 3D full wave STELEC (stellarator_ECH, tokamaks included as particular case) code [1]. Code includes all basic wave physics as interference, diffraction, wave tunnelling, mode conversion at Upper Hybrid resonance (UHR) to electron Bernstein waves and appropriate boundary conditions. Code operates in real 3D magnetic geometry and uses massive parallel terabyte computers and firstly permitted solution of above problem. In this paper the reflection, refraction and diffraction effects are investigated at second harmonic and these are shown to be important even at moderate plasma densities.

1. Second Harmonic ECH Scenarios in T-10

Majority of present tokamaks and stellarators operate at second harmonic and for not so large plasma densities the UHR is absent one. Second harmonic X-mode launch in T-10 is shown in Fig.3a: |real(E_psi)|, at N=90 ($N_{//}(0)=0.02$), F=140 GHz, $N_e(0)=4.5\times10^{19}$ m^{-3}, Te(0)=8.7 kV, ($\alpha_n=1$, $\alpha_T=2$), Bo=2.5 T, Ip=300 kA (relativistic effects are included) and power deposition is displayed in Fig.3b.

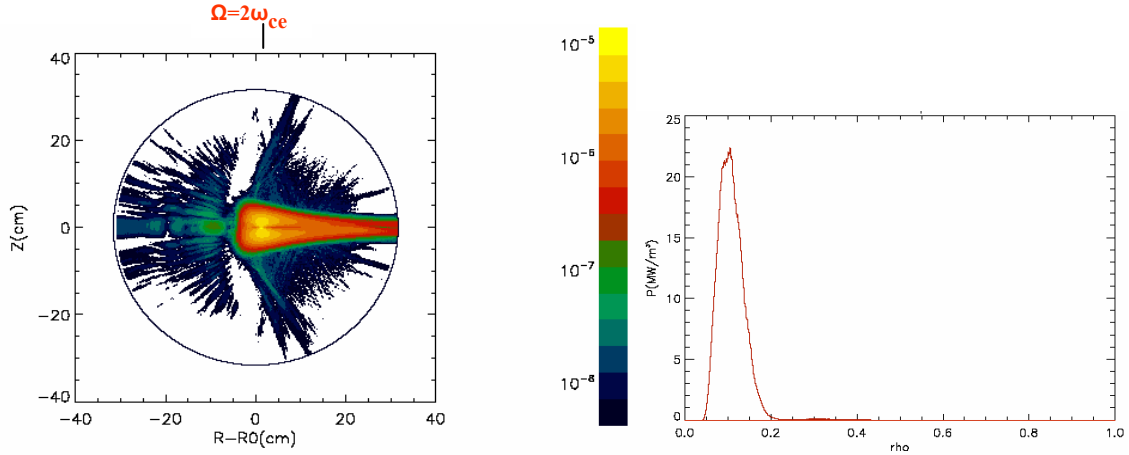

FIG.3a *|real(E_psi)| in T-10, $N_e(0)=4.5\times10^{19}$ m^{-3}* FIG.3b *$P_e(\rho)$ in T-10, $\omega= 2\omega_{ce}$, F=140GHz*

At plasma density $N_e(0)=9\times10^{19}$ m^{-3} the diffraction is more strong one (Figs.4a,b).

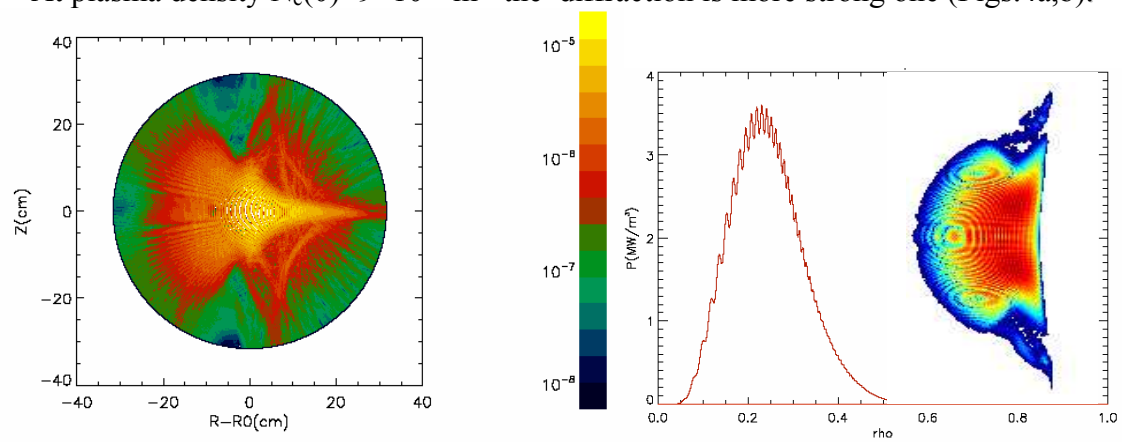

FIG.4a *|real(E_psi)| in T-10, $N_e(0)=9\times10^{19}$ m^{-3}* FIG.4b *1D&2D P_e in T-10, $N_e=9\times10^{19}$ m^{-3}*

2. Second Harmonic ECH Scenarios in DIII-D at Oblique Launch

Second harmonic X-mode oblique 1 MW upper port launch in DIII-D **H-mode dense** plasma with elongation κ=1.65, triangularity δ= 0.5, N=160 (N//(0)=0.075), F=60 GHz, T_{e0}=6.55 kV, $N_e(0)=1.0\times10^{19}$ m^{-3} , Ip=360 kA, B_o= 0.95T, q(0)=1.1, q(a)=5.4 is displayed in Figs.5a,b by |real(E_psi| and |Im(E_z)| fields components.

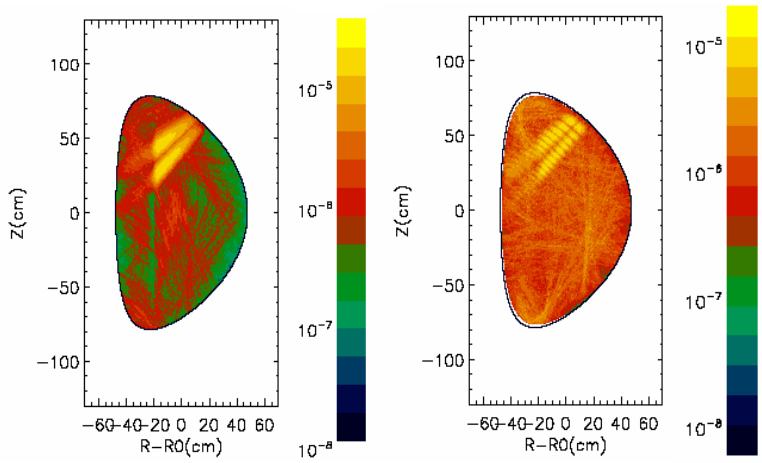

Radial power deposition calculated by STELEC for elliptically polarized Gaussian X- antenna is given by Fig.6 One can see two wave patterns propagation and absorption lobs. Standing wave structure, clearly seen on E_z contour plots, shows that the reflection and diffraction effects play a remarkable role in dense plasma H-mode scenario.

FIG.5a |*real(E_psi) |in DIII-D at* $2\omega_{ce}$ FIG.5b |*Im(E_z)| in DIII-D at* $2\omega_{ce}$

In DIII-D **L-mode rare** plasma with $N_e(0) = 0.5\times10^{19}$ m^{-3} , B_o= 1.05T, with smaller density gradients, the wave reflection plays a smaller role as displayed by Figs.7a,b.

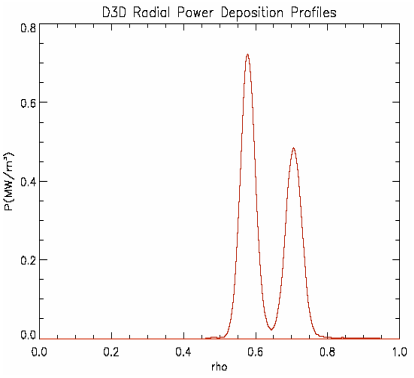

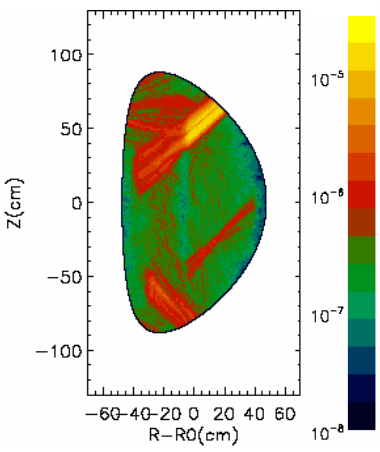

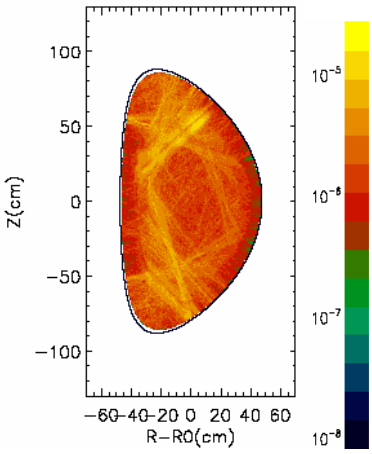

FIG.6 $P_e(\rho)$ *in DIII-D calculated by STELEC* FIG.7a |*real(E_psi) |in DIII-D* FIG.7b |*Im(E_z)| in DIII-D*

In DIII-D **L-mode dense** plasma with $N_e(0) = 2.0\times10^{19}$ m^{-3} ($N_e(0) \sim N_{cr}$) the diffraction and refraction effects are more pronounced as is demonstrated by |real(E_psi| and |Im(E_z)| fields components in Figs.8a,b.Radial power deposition for this case is given by Fig.9. One can see two wave patterns propagation and triple absorption lobs. Wing lobs are remarkably smaller ones. Behavior of parallel E_z contour plots shows that the O-mode more deeply propagates beyond second harmonic resonant zone with following multiple reflections from the walls

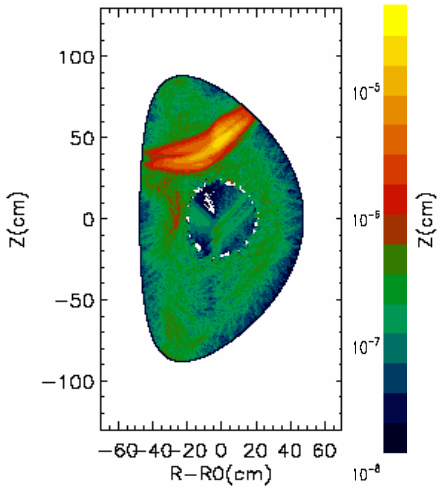

FIG.8a *|real(E_psi) |in DIII-D at* $N_e(0) = 2.0\times10^{19}\ m^{-3}$

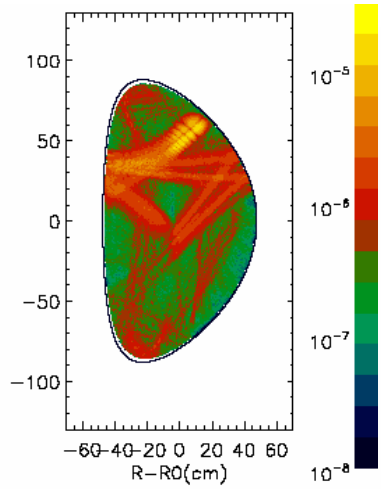

FIG.8b *|Im(E_z)| in DIII-D at* $N_e(0) = 2.0\times10^{19}\ m^{-3}$

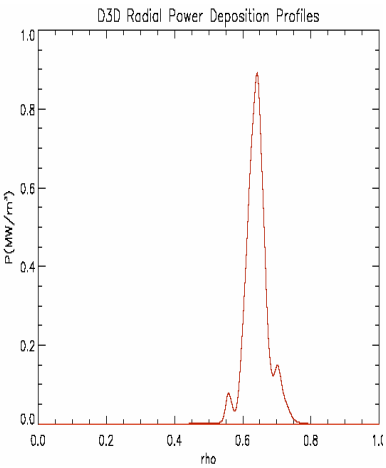

FIG.9 $P_e(\rho)$ *in DIII-D, at* $N_e(0) = 2.0\times10^{19}\ m^{-3}$

3. ECH Similarity Laws check for ITER

This was done for the ITER hydrogen phase of operation at twicely reduced magnetic field for scenario #2, i.e. at second harmonic X-mode outside launch from the upper port. at Bo=2.65 T for F = 5, 10.1, 20.2 and 30.3 GHz with the gaussian beam divergence ±0.71° and $N_{//} = 0.09$ suitable for NTM suppression scenario. The 2D contour plots of electrical fields |Re(E_psi)| are given by Fig.10 and displaying very similar wave pattern for all frequencies.

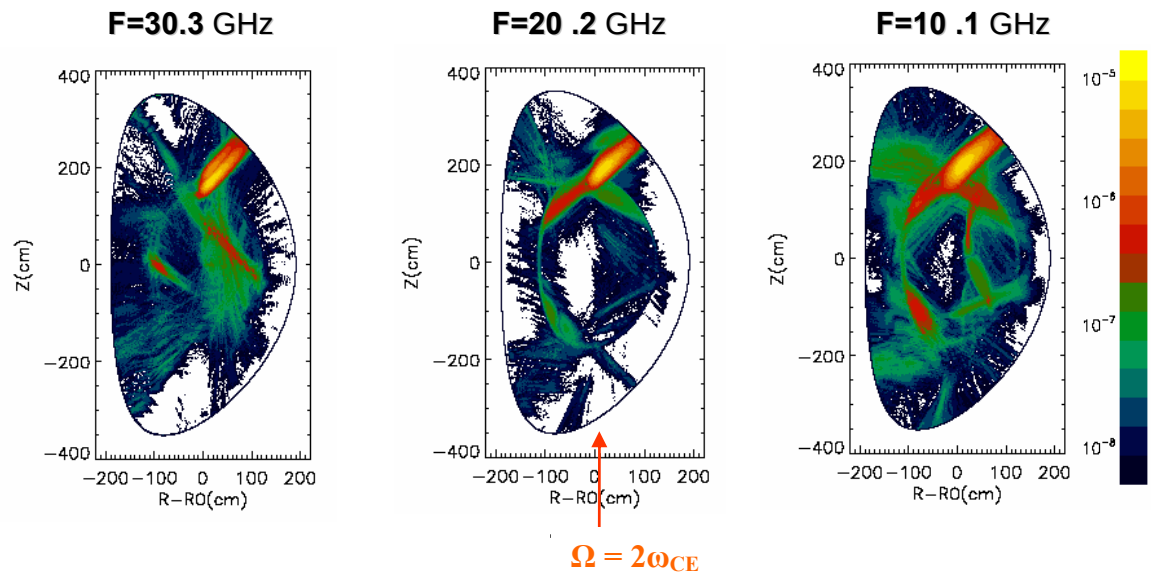

Fig.10 *Contour plots of |Re(E_psi)| for three frequencies in non active ITER*

The respective flux surface averaged radial power deposition profiles are shown at Figs.11a,b,c. They are also very similar and displaying well localized power deposition profiles in conditions of absence into plasma Upper Hybrid resonance. Thus ECH similarity Laws [1] are working well as shown for the frequency change up to factor ~6.

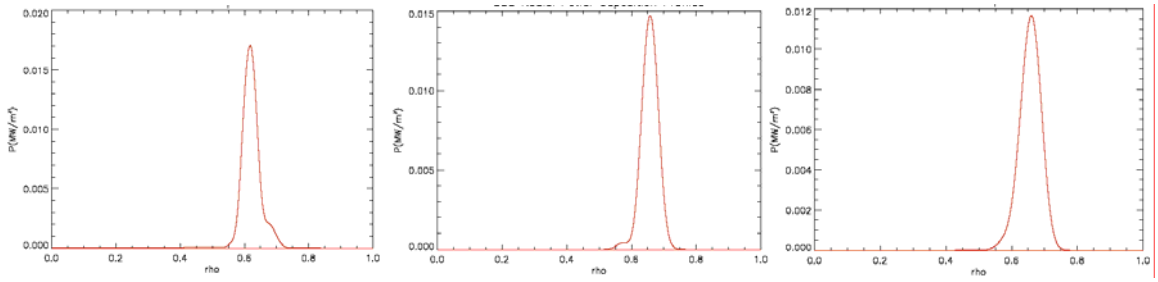

Fig.11a P_e in ITER at 30.3 GHz *Fig.11b Pe at 20.2 GHz* *Fig.11c Pe at 10.1 GHz*

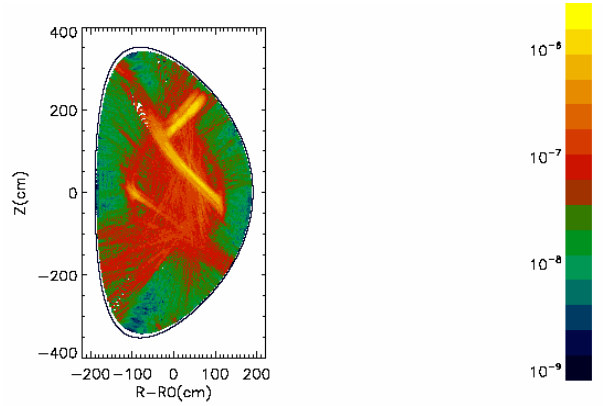

FIG.12 *|Im(E_z)| in ITER*

The Fig.12 shows parallel electrical fields |Im(E_z)| at second harmonic in the ITER: The remarkable reflection from second harmonic resonance layer at 30.3 GHz is evident one. (DIII-D earlier modelling has shown similar effect at 44 GHz [1]])

Conclusions

In toroidal bounded plasmas the O-mode and X-mode are coupled ones through the space inhomogenity and boundary conditions even at second EC harmonic. This modes coupling effect in toroidal plasmas is weak one but important at the second harmonic scenarios in waves reflecting conducting chamber. In second harmonic scenarios the modes coupling is more weak one. Ray tracing/bi-tracing technique may be still used.

Second harmonic X mode scenarios in T-10, DIII-D and ITER evidently show more broader power deposition profiles in compare with usual ray tracing ones at moderate plasma densities. At low densities the ray tracing approach still works. Refraction and diffraction effects in rare and dense plasmas were modelled for the T-10 and DIII-D tokamaks in circular and elongated magnetic configurations respectively.

Recent STELEC code modelling for non active ITER phase plasma in frequency range 5 – 30 GHz confirmed validity for the similarity laws use at reduced frequencies for large fusion machines.

References

1. Vdovin V.L. *Role of Upper Hybrid resonance and diffraction effects at Electron Cyclotron Heating in tokamaks* , Proceedings of 14th Joint Workshop on Electron Cyclotron Emission and Electron Cyclotron Resonance Heating, invited lecture, p.323-333, 9 - 12 May 2006, Santorini island, Greece (Publisher: Heliotopos Conferances Ltd., Athens, Greece; ISBN: 960-89228-2-8, December 2006)